Proceedings of the 21st ICSMGE, Vienna, Austria, 14 – 19 June 2026. Pistrol, Adam & Schweiger (eds.)
Published by: ÖGG, Austrian Society for Geomechanics, Salzburg, Austria, ISBN 978-3-9503898-4-5
https://doi.org/10.53243/ICSMGE2026-2295

Experimental study on the seismic behavior of reinforced leaning-type retaining walls focusing on the effect of soil nail deformation

Keita Abe, Noriaki Sento
College of Engineering, Nihon University, Japan, abe.keita@nihon-u.ac.jp

ABSTRACT: This study investigates the seismic reinforcement of leaning retaining walls that have experienced severe damage during earthquakes. Reinforcement is typically achieved using the soil nailing method, in which multiple soil nails composed of reinforcing bars and mortar are installed on the wall. However, current design approaches often neglect the deformation of these soil nails, even though they can generate tension forces and bending moments owing to wall displacement during earthquakes. The objective of this study is to clarify how soil nail deformation affects these forces and the seismic behavior of the wall. To achieve this, static loading and shaking table tests were performed using a 1/10-scale model of a leaning retaining wall, both before and after reinforcement. The experiments examined the relationship between the soil nail deformation and overturning and sliding modes of the wall. The results revealed that the soil nails deformed into an upward convex shape regardless of the installation depth, producing bending moments opposite to the direction of the wall inclination. Tension forces and bending moments were more prominent during overturning than during sliding. Notably, the bending moment from the deformed nails affected the seismic behavior and stability of the wall. When the nails were installed only in the upper part, their influence on the overturning mode became particularly evident. These findings highlight the importance of considering soil nail deformation in design, enabling a more rational evaluation of their stabilizing effects and contributing to more effective seismic reinforcement strategies for leaning retaining walls.

KEYWORDS: Leaning retaining wall, soil nailing reinforcement method, seismic behavior.

1 INTRODUCTION

The seismic reinforcement of leaning retaining walls that have suffered severe damage such as overturning during past earthquakes has conventionally been performed using the soil nailing reinforcement method, in which multiple soil nails are installed on the wall (Nakajima et al., 2019). However, current design practices do not consider the effects of the deformation of these soil nails as part of their reinforcing performance (e.g., JGS, 2011). During earthquakes, a leaning retaining wall undergoes displacement, which can cause the soil nails themselves to deform. This deformation can generate tension forces and bending moments opposite to the wall inclination direction, thereby influencing its seismic behavior. To investigate this effect, a series of static loading and shaking table tests were conducted using 1/10-scale models of leaning retaining walls before and after reinforcement. The experiments focused on how the deformation of soil nails influences the tension forces, bending moments, and seismic behavior of the wall, which consists of overturning and sliding. This paper presents the experimental details, results, and a discussion.

2 OVERVIEW OF STATIC LOADING TESTS

Static loading tests were conducted to investigate the effects of wall inclination and sliding on the tension forces and bending moments generated by the deformation of soil nails. Figure 1 shows a cross-sectional view of the test model. The model simulated a leaning retaining wall with a height of 5.0 m that was reinforced using soil nails. A 1/10-scale wall model was made of aluminum with a hinge fixed at the bottom that had a height of 600 mm, width of 20 mm, and depth of 390 mm. Two soil nail models, 360 mm in length and 10° in the depth direction, were inserted 180 mm and 475 mm from the top of the wall. The interval between the soil nail models in the depth direction was 200 mm.

Strain gauges were attached to the upper and lower surfaces of each soil nail at distances of 40 mm, 110 mm, and 180 mm from the rear face of the wall. A uniaxial load cell was installed at the head of each soil nail to measure the tension forces. The backfill material was silica sand No. 5 ($\rho_s = 2.65$ Mg/m³, $e_{max} = 0.85$, $e_{min} = 0.53$, $U_c = 1.65$, $U_c' = 1.30$, $\rho_d = 1.49$ Mg/m³, $w = 0.24$–0.45%, $c_{peak} = 1.92$ kN/m², $\phi_{peak} = 32.1°$, $c_{res} = 2.22$ kN/m², and $\phi_{res} = 30.0°$), which was compacted in 50-mm-thick layers to form the backfill. A 1.0 kN/m² surcharge scaled to 10.0 kN/m² in the prototype was modeled by placing crushed stone with a 15 mm diameter on top of the backfill.

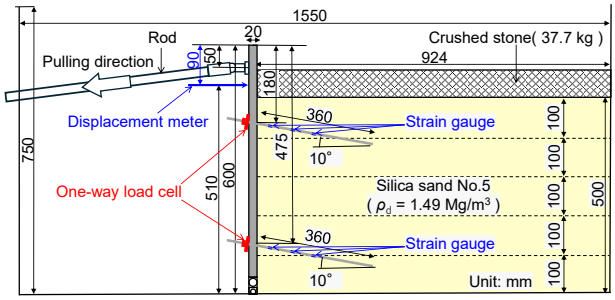

Figure 1. Cross-section of static loading test model.

The soil nail models were hollow aluminum rods that were coated with silica sand to model circumferential friction. The bending stiffness of an actual soil nail with an outer diameter of ϕ100 mm and a core diameter of ϕ25.4 mm is $E_pI_p = 1.69 \times 10^5$ Nm². The corresponding scale-converted bending stiffness was calculated as 5.34 Nm², based on the similarity law with a similarity ratio $\lambda = 3.2 \times 10^4$ (Iai, 1989). The bending stiffness of a hollow aluminum pipe with an outer diameter of ϕ8.0 mm and inner diameter of ϕ7.0 mm is $E_mI_m = 5.80$ Nm², which is close to the scale-converted bending stiffness of an actual soil nail. Therefore, a hollow aluminum pipe was selected as the soil nail model. The deformation modulus ratio between the backfill and soil nail E_{s_m} / E_m is 3.0×10^{-4}, where the deformation modulus of the backfill $E_{s\_m} = 5.0 \times 10^3$ kN/m². This value corresponds closely to the deformation modulus ratio of the prototype $E_{s\_p} / E_p = 2.3 \times 10^{-4}$, where the deformation modulus of the actual backfill, which is assumed to be a sandy soil with $N \approx 11$ corresponding to $\phi = 30°$, $E_{s\_p} = 7.9 \times 10^3$ kN/m².

In the tests, the wall model was inclined at an angular velocity of 0.003°/s using two rods attached 50 mm below the top of the wall. The inclination angle was measured using a contact-type displacement gauge located 90 mm from the top. The horizontal sliding tests were also conducted at a horizontal velocity of 0.04 mm/s, with two rods added to the bottom of the

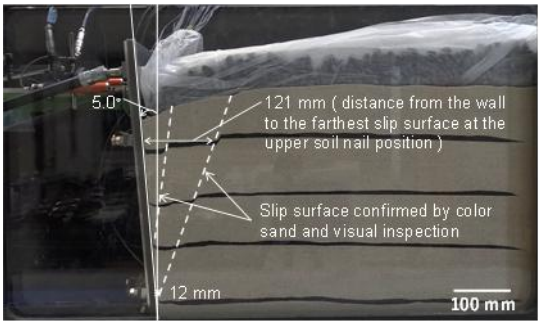

Figure 2. Situation at an inclination angle of 5.0°.

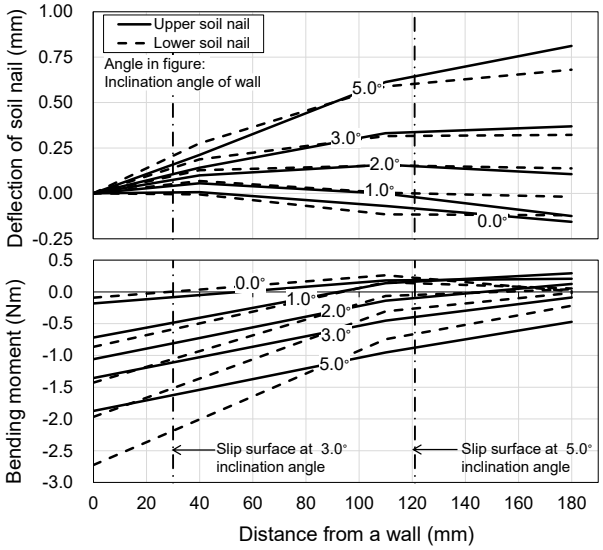

Figure 3. Deflection profiles and bending moment distributions of the soil nail models.

wall, to compare the tension forces and bending moments between the inclined and sliding conditions.

3 RESULTS AND DISCUSSION OF STATIC LOADING TESTS

Figure 2 shows the conditions of the model at an inclination angle of 5.0°. As the wall tilted, an active failure mechanism occurred, forming a wedge-shaped sliding soil mass in the backfill. Figure 3 shows the deflection profiles and bending moment distributions of the soil nail models at each inclination angle. A positive moment indicates tension at the bottom and compression at the top. The deflection profiles were obtained by integrating the bending strains obtained from the strain gauges. The bending strain was divided by the distance from the neutral axis to the outer edge, that is, the radius of the soil nail. Double integration was then performed using the distances from the wall to each strain gauge, as well as between the gauges. The bending moment distributions were calculated by multiplying the bending strain by the bending stiffness and inverse of the soil nail radius. The bending moment at 0 mm from the wall was estimated by linearly extrapolating the values at 40 mm and 110 mm, assuming that the soil nail remained within the elastic range. The maximum bending strain and axial strain observed up to a 5° inclination were approximately 1500 μ and 100 μ, respectively—both below the yield strain of 2000 μ. Similar results were observed for all tested soil nail models.

The deflection profiles indicated that, regardless of the installation depth, the soil nail models deformed into an upward convex shape as the wall tilted. This deformation is considered to have occurred because, as the wall tilted, the connection

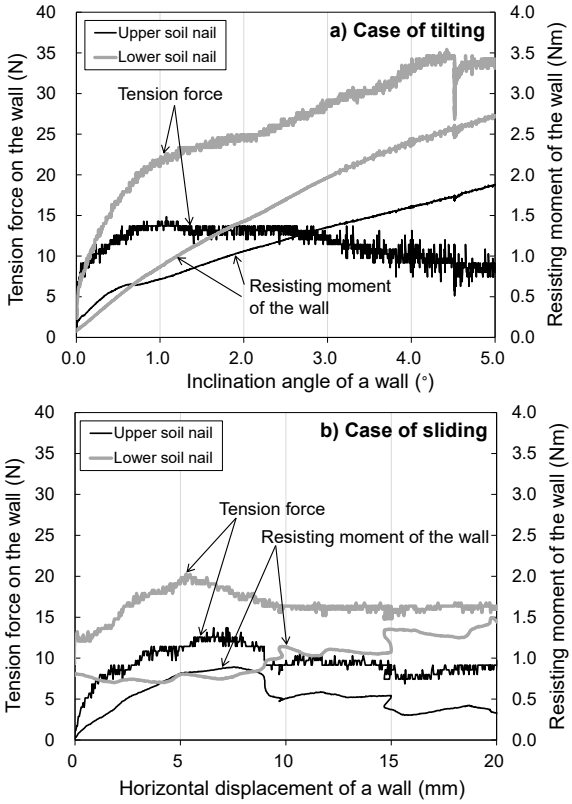

Figure 4. Relationship between tension force and resisting moment versus wall inclination angle and horizontal displacement during wall tilting and sliding.

point between the soil nail and wall moved downward, whereas the distal end of the soil nail embedded in the backfill tended to remain fixed within the backfill. The visually identified slip surface positions at inclination angles of 3° and 5° are shown in Figure 3. The noticeable difference in the deflection across the slip surface implies that the formation of the slip surface influenced the change in the shape of the soil nails. The bending moment distributions indicate that as the soil nails deformed into an upward convex shape, the bending moment at 0 mm from the wall became significantly negative. This indicates that positive bending acted on the wall, implying that the soil nails exerted a bending moment in the direction opposite to the inclination of the wall. Hereafter, the bending moment is referred to as the resisting moment.

Figure 4 shows the relationship between the tension force and resisting moment versus the wall inclination angle and horizontal displacement during wall tilting and sliding. The results indicate that the resisting moment increased with the inclination angle during tilting, whereas it exhibited little variation during sliding. Most of the resisting moments of the lower soil nail during sliding occurred at a displacement of 0 mm. In addition, the deflection profile remained almost unchanged during sliding. In fact, the maximum bending and axial strains in the soil nails during sliding were approximately 400 μ and 250 μ, respectively. This implies that the bending deformation of the lower soil nail observed during sliding was primarily induced during the initial backfill preparation. In actual construction, where soil nails are inserted from the front face of the wall, such initial bending deformation is unlikely to occur. Therefore, it is considered that the resisting moment owing to the deformation of the soil nail during sliding was negligible compared to that during tilting.

The results indicate that the tension force was greater during tilting than during sliding, with a noticeable increase in

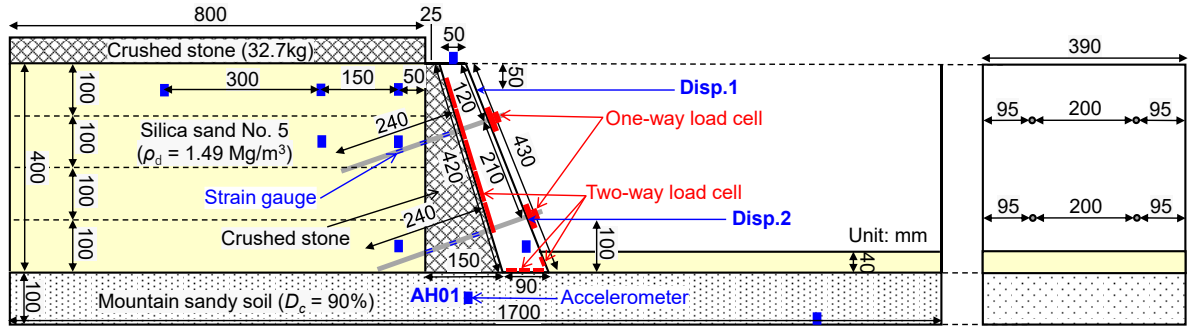

Figure 5. Cross-section and front view of shaking table test model (Case 3).

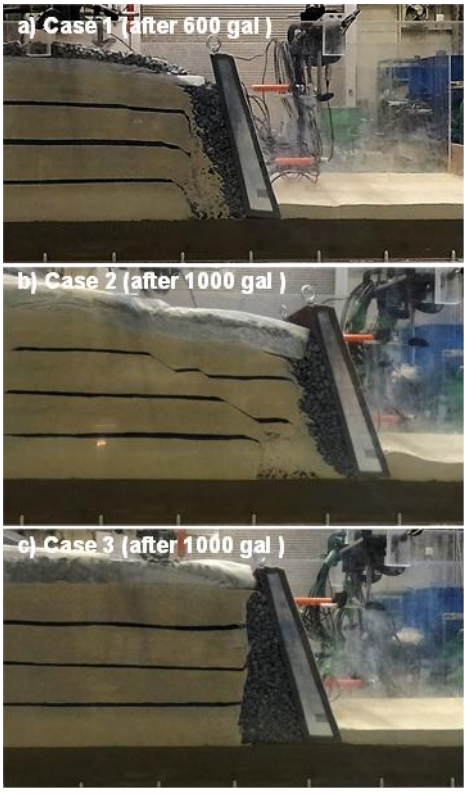

Figure 6. Conditions of the model after shaking.

the tension force of the soil nails that were installed in the lower portion of the wall as the inclination angle increased. This is likely owing to changes in the mobilization of interface friction along the soil nail surface caused by upward convex deformation during wall tilting. The detailed mechanism of the tension force generation requires further investigation.

4 OVERVIEW OF SHAKING TABLE TESTS

A series of shaking table tests were conducted to investigate the effects of the tension forces and resisting moments generated by the soil nails on the seismic behavior of leaning retaining walls. Figure 5 shows a cross-section and front view of the test setup for Case 3. The experiment was performed using a shaking table with a 2.0 m length and 2.0 m width owned by the College of Engineering, Nihon University, Japan. An acrylic soil container with a 1800 mm length, 600 mm height, and 400 mm width was placed on the shaking table and the test model was constructed inside.

The test model made of aluminum represents a 1/10-scale leaning retaining wall with a height of 4.0 m, with a height of 400 mm, width of 50–90 mm, and depth of 390 mm. Sandpaper with grit size #80 was attached to the back, bottom, and front faces of the wall model to model the interface friction. Three cases were tested: an unreinforced wall (Case 1) and two reinforced walls (Cases 2 and 3). Soil nail models identical to those in the static loading tests, that is, hollow aluminum rods with a length of 316 mm, an embedded length of 240 mm, an outer diameter of ϕ8.0 mm, and an inner diameter of ϕ7.0 mm, were used. In Case 2, two soil nail models were installed in the upper part of the wall model, 112 mm from the top, angled downward at 21.4°, spaced 200 mm apart, and inserted 95 mm away from the side walls of the soil container. In Case 3, two additional soil nails were installed in the lower part, 100 mm above the base. Finally, the wall model was reinforced with four soil nails in Case 3.

The horizontal displacement and inclination angle of the wall were measured using contact-type displacement gauges placed on the upper and lower parts of the front face. The earth pressure and base and front reaction forces were measured using bidirectional load cells: five at the back, three at the base, and two at the front of the wall. Accelerometers were installed in the supporting soil and backfill and on the wall to record the ground motion and inertial forces. Strain gauges were attached to the upper and lower surfaces of each soil nail at distances of 24 mm, 74 mm, and 124 mm from the wall to measure the bending and axial strains.

The backfill was made of silica sand No. 5 at the same density as in the static loading test (ρ_d = 1.49 Mg/m³, w = 0.64%–0.98%). The supporting soil was mountain sand with a degree of compaction D_c = 90.0% (ρ_s = 2.73 Mg/m³, U_c = 44.0, D_{50} = 0.70 mm, F_c = 15.0%, ρ_{max} = 1.93 g/cm³, w_{opt} = 12.9%, and w = 6.4%–6.5%). Both soils were compacted in 50 mm layers with controlled density. Crushed stone with 15 mm in representative diameter and 1.54–1.57 Mg/m³ in density was placed between the wall and backfill to model gravel backfill. Crushed stone was also placed at the top of the backfill to model a surcharge of 1.0 kN/m² scaled to 10.0 kN/m² in the prototype.

Sinusoidal waves of 5 Hz and 10 cycles were applied as the input motion for all models, with the amplitudes gradually increasing in about 50 gal increments, considering the similarity laws (Iai, 1989). In Case 1, shaking was applied up to a maximum of 600 gal, whereas in Cases 2 and 3, shaking was applied up to 1000 gal in a single direction.

5 RESULTS AND DISCUSSION OF SHAKING TABLE TESTS

Figure 6 shows the conditions of the model after shaking. In Case 1, the heel of the wall base was lifted because of shaking, causing the wall to return to an upright position. In Cases 2 and 3, both the displacement and inclination angles were smaller

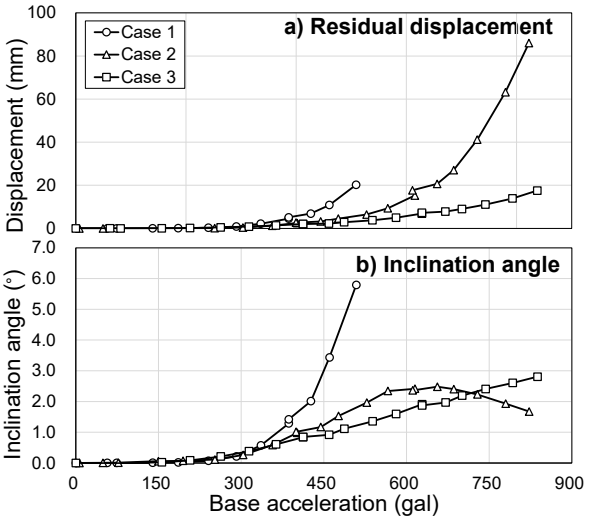

Figure 7. Relationship between the peak value of the base acceleration and the horizontal displacement and inclination angle of the wall at the base with a positive in the forward direction.

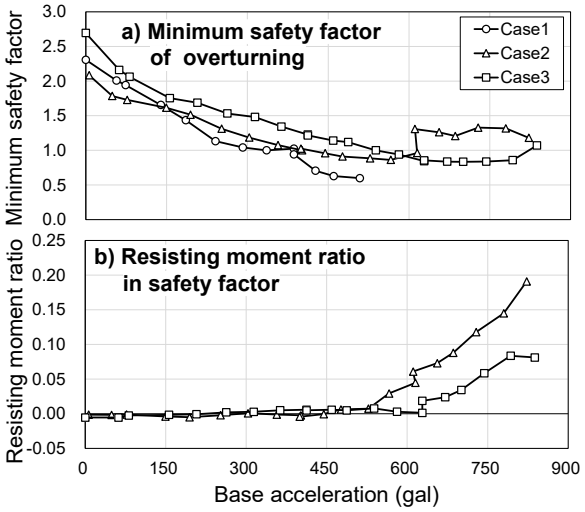

Figure 9. Relationship between the base acceleration and minimum overturning safety factor and resisting moment ratio in the safety factor.

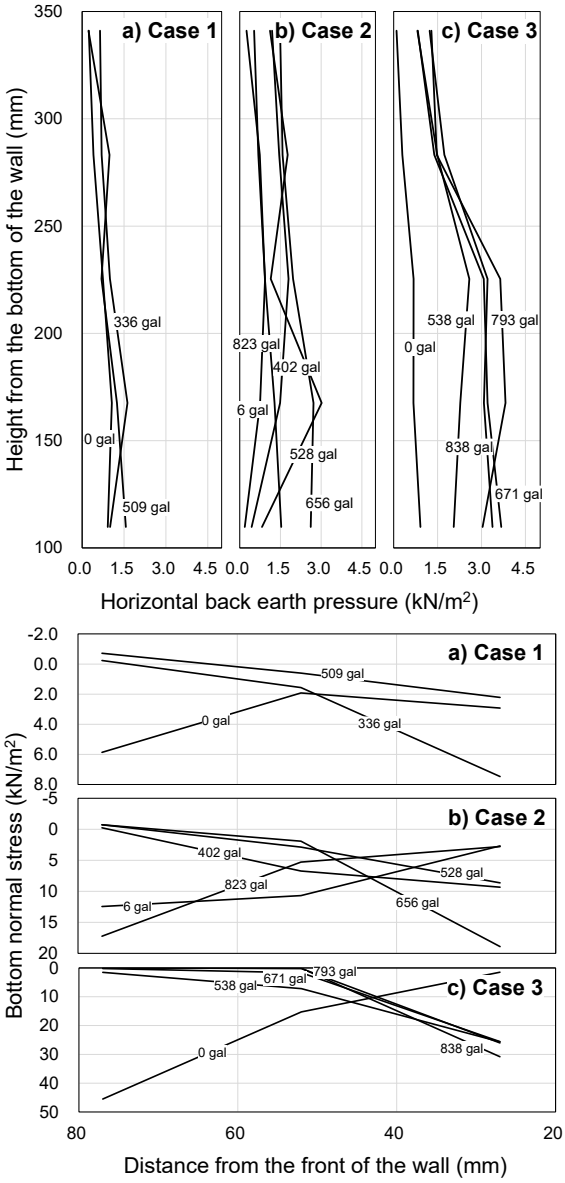

Figure 8. Distribution of back earth pressure with a positive in the forward direction and base soil reaction with a positive upward when the minimum overturning safety factor occurred during shaking.

than those in Case 1, indicating the effectiveness of the reinforcement. Figure 7 shows the relationship between the peak value of the base acceleration measured by AH01 and the horizontal displacement at the lower part and inclination angle of the wall, which was positive in the forward direction. In Case 1, the displacement and inclination started to increase at 200 gal and then increased rapidly. In contrast, although Cases 2 and 3 showed increases from 200 gal, the rate of increase was much more gradual. In Case 2, the inclination angle peaked at approximately 600 gal and then started to decrease, indicating that the wall had started to tilt backwards.

Figure 8 shows the distribution of the back earth pressure with a positive in the forward direction and base soil reaction with a positive upward when the minimum overturning safety factor occurred during shaking. The back earth pressure increased progressively from Case 1 to Case 3, corresponding to improved wall fixation. As the wall tilted, the base reaction force shifted towards the front edge, causing the heel to lift. The heel reaction was zero at 336 gal in Case 1, 402 gal in Case 2, and 538 gal in Case 3. Based on the design guidelines in Japan (e.g., MLIT and RTRI, 2012), these points are considered to correspond to a safety factor of 1. Figure 9a shows the relationship between the peak value of base acceleration and minimum overturning safety factor when the abovementioned points were set to a safety factor of 1. In Cases 2 and 3, the safety factor included the effects of tension forces and resisting moments from the soil nails. Although Case 3 exhibited a higher initial safety factor, both cases showed a generally similar decreasing trend as the shaking increased. Notably, in Case 2, the safety factor recovered when the base acceleration was approximately 600 gal, corresponding to the point at which the wall began to tilt backward.

Figure 10 shows the deflection profile and bending moment distributions of the upper soil nails in Cases 2 and 3, respectively. Up to 700 gal, the maximum bending and axial strains remained below 2000 μ. In Case 2, upward convex deformation became dominant at approximately 600 gal, with increasingly negative bending moments. In Case 3, similar changes were observed at approximately 700 gal. It was

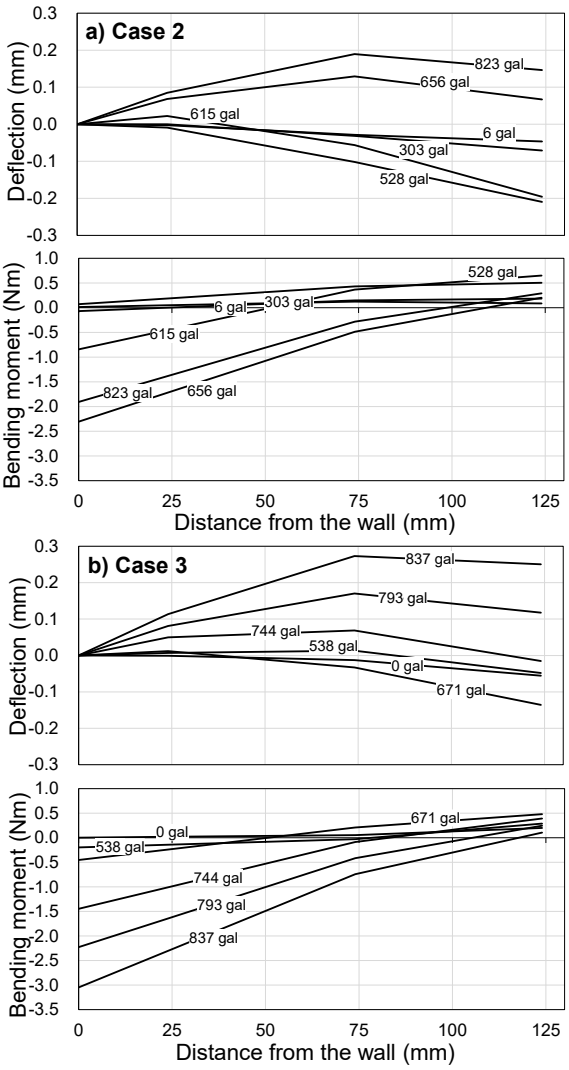

Figure 10. Deflection profile and bending moment distributions of the upper soil nails in Cases 2 and 3.

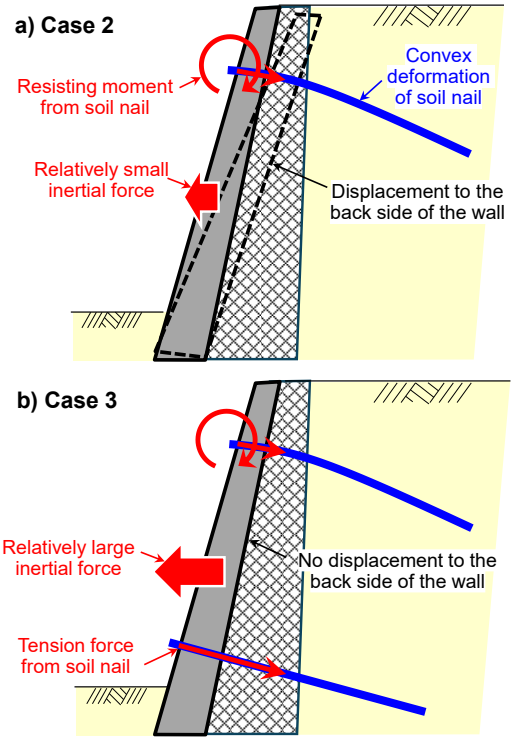

Figure 11. Schematic of influence mechanism of influence of the resisting moment owing to deformation of the soil nails and tension force on the seismic behavior of the wall in Cases 2 and 3.

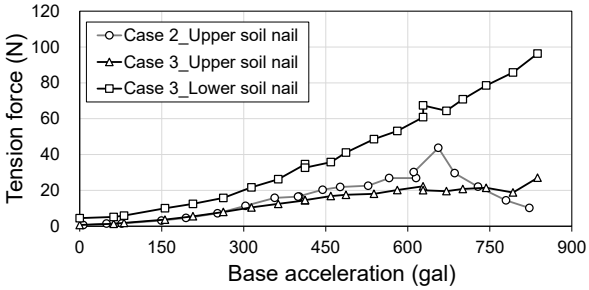

Figure 12. Relationship between base acceleration and tension force at the point of the minimum overturning safety factor.

confirmed that the deflection and bending moments of the lower soil nails in Case 3 were minimal in terms of both magnitude and variation. These results indicate that in Case 2, the bending deformation of the soil nails, and thus, the generation of resisting moments, occurred earlier than in Case 3. Figure 9b shows the contribution ratio of the resisting moment to the overturning safety factor for each peak value of base acceleration. This also confirms that the resisting moments were mobilized earlier in Case 2.

Based on the above results, the mechanisms of seismic behavior shown in Figure 11 can be considered. The convex deformation of the soil nails in Case 2 occurred earlier than in Case 3, generating resisting moments that acted on the wall. This caused the wall to tilt backwards, resulting in a reduced forward inclination angle and an increase in the minimum overturning safety factor. Based on the results of the static loading tests, the development of resisting moments is highly dependent on the inclination of the wall. Therefore, because the wall in Case 2 was inclined earlier than that in Case 3, the resisting moments from the upper soil nails were mobilized at a relatively early stage when the inertial force of the wall was still small. This early mobilization may have influenced the shift in the inclination mode of the wall.

Figure 12 shows the relationship between the peak value of base acceleration and tension force at the point of the minimum overturning safety factor. In Case 2, the tension force increased with the base acceleration but started to decrease near the point where the wall tilted backward. In Case 3, the tension force in the upper soil nails increased, similar to Case 2. However, the tension force in the lower soil nails increased significantly. This implies that the lower soil nails provided a stronger anchoring effect in Case 3, holding the wall in place. In contrast, the absence of this effect in Case 2 allowed the lower part of the wall to move forward, leading to a dominant backward tilt. The passive earth pressure on the front face of the wall generally remained low. Therefore, it was considered to have a minimal effect. These results indicate that if the resisting moment owing to the deformation of the soil nails and the anchoring effect at the base of the wall are properly considered in the design, it may be possible to evaluate the improvement in overturning safety more rationally, even in cases with relatively few soil nails, as observed in Case 2. However, the occurrence of these phenomena depends on the specific properties of the walls and soil nails. In addition, although this study focused primarily on overturning, the actual design must also consider

horizontal wall displacement, backfill deformation, and internal stresses within the wall body. These aspects should be examined further in future studies. In addition, the influence of the soil nail deformation on the tension force was not explicitly addressed in this study. Clarifying this influence in future studies may lead to a more rational and accurate evaluation of the tension force in the design.

6 CONCLUSIONS

In this study, model experiments were conducted on leaning retaining walls before and after reinforcement using soil nails to investigate the effect of the deformation of the soil nails on the tension forces, resisting moments, and seismic behavior of the wall. The main findings are as follows:

1. The soil nails deformed into an upward convex shape regardless of their installation position, generating a bending moment opposite to the direction of the wall inclination.
2. Both the tension forces and bending moments were more prominent during overturning than during sliding.
3. The bending moment from the soil nails affected the seismic behavior and overturning safety factor of the wall. In particular, when soil nails were installed only on the upper part of the wall, it is possible that they influenced the overturning mode.

These findings imply that the reduction effect of wall inclination owing to soil nails can be evaluated more rationally when the effect of soil nail deformation is considered. It is essential to examine how these findings can be incorporated effectively into design practices in the future.

7 ACKNOWLEDGEMENTS

This work was supported by JSPS KAKENHI (Grant Number 23K04032). The authors would also like to express their sincere gratitude to Dr. Susumu Nakajima of the Railway Technical Research Institute in Japan, Mr. Masatoshi Iijima of the Integrated Geotechnology Institute Limited in Japan, and former students of the College of Engineering, Nihon University in Japan—Mr. Kenshiro Anzai, Mr. Yuki Oya, Mr. Yoshihiko Sato, Mr. Shouga Sawaki, Mr. Yuki Fukuchi, and Mr. Mitsuki Yoshida—for their assistance with the experiments.

8 REFERENCES

Iai, S. 1989. Similitude for shaking table tests on soil-structure-fluid model in 1G gravitational field. Soils and Foundations 29(1), 105-118.

Japanese Geotechnical Society (JGS), 2011. Design and Construction Manual for Soil Nailing. Maruzen Publishing (in Japanese).

Nakajima, S., Kudo, A., Narita, H. and Watanabe, K. 2019. Experimental study on effect and design methodology of aseismic reinforcement for existing leaning type retaining wall. *Journal of the Japan Society of Civil Engineers, Ser. C* (*Geosphere Engineering*) 75(3), 316-335 (in Japanese).

The Ministry of Land, Infrastructure, Transport and Tourism (MLIT, Supv.), the Railway Technical Research Institute (RTRI, Ed.), 2012. *Design Standards for Railway Structures and Commentary* (*Foundation*). Maruzen (in Japanese).